Proposal to Fermilab

Neutrino Physics

R. Fine, S. Holmes, W. Lee,* R. Seto, P. Sokolsky

Columbia University, New York, N.Y. 10027

M. Lamm, T. O'Halloran, Jr., C. Olsewski, J. Wiss

University of Illinois, Urbana, Ill. 61801

H.P. Parr

NIKHEF-H, Amsterdam, Holland

* Spokesperson.

May 1979

Introduction

The present generation of neutrino experiments, which were born in the early 70's, have contributed immensely to our current understanding of the weak interactions. These experiments have all lent support to an interpretation in terms of the Weinberg-Salam (W-S) model of weak interactions and the quark-parton description of nucleons. More recently, measurement of the purely leptonic reaction, $\nu_\mu + e^- \rightarrow \nu_\mu + e^-$, has provided a test of the W-S model independent of strong interaction dynamics.

In early 1978, a series of beam dump experiments were performed utilizing the BEBC, Gargamelle, and CDHSB detectors at CERN. The two bubble chamber experiments measure a ratio of neutrino-induced electron events to neutrino-induced muon events much larger than what is expected of neutrinos from conventional sources, while the CDHSB detector observes an anomolously large ratio of neutral current to charged current events. The BEBC detector also measures this effect at 15 mr with respect to the incident proton direction and sees an even greater enhancement of electron events relative to muon events than at 0 mr. These data indicate the existence of a new source of neutrinos which produces approximately equal numbers of electron neutrinos and muon neutrinos. Such a source is believed to be charmed particles produced in p-p collisions which then decay leptonically.

We propose an experiment to measure the interactions of prompt neutrinos produced in a beam dump. We expect that by looking in regions away from 0 mr we will have approximately equal numbers of ν_e, $\bar{\nu}_e$, ν_μ, and $\bar{\nu}_\mu$ passing through our detector. The production and decay of F mesons will provide us with a usable source of tau neutrinos. The detector we propose is designed to emphasize the study of the previously unmeasured processes involving electron neutrinos and tau neutrinos:

1) $\nu_e(\bar{\nu}_e)+e^- \rightarrow \nu_e(\bar{\nu}_e)+e^-$

and

2) $\nu_\tau+N \rightarrow \tau+\text{anything}$.

The detector will consist of three units: an electron detector to measure the elastic scattering of neutrinos off electrons, a neutrino detector to measure deep inelastic neutrino scattering, and a muon detector to measure the muon associated with the neutrino. The muon detector will be used to tag ν_τ interactions in the neutrino detector using a sign correlation to be described later and can also be used in conjunction with the neutrino detector to search for new sources of $\mu\nu$ pairs.

Calculation of Neutrino Fluxes and Detector Layout

In calculating sources of prompt neutrinos, we are guided by the CERN beam dump results at 0 mr and 15 mr.[1,2] The major source of such neutrinos is the production of charm. We have followed the production model of Bourquin and Gaillard[3] to describe the production of D mesons and have extended it to describe the F. We use a production cross section for the D which is consistent with the BEBC 15 mr result. For F production, we use, $\sigma \cdot B(F)/\sigma \cdot B(D) = 1/10$, [4] where B(F) describes the decay $F^+ \to \tau^+ \nu_\tau$ and B(D) describes $D \to \mu^+ \nu_\mu K$. Although there is no conclusive experimental evidence for the existence of the fifth and sixth quarks, they are universally believed to exist. For the sake of discussion, we have again extended the model of Bourquin and Gaillard to describe the production of 5 GeV bottom mesons. Although the production cross section is unknown, we use the value $\sigma \cdot B(B)/\sigma \cdot B(D) = 1/100$ where $\sigma \cdot B(B)$ describes the decay, $B \to D\mu\nu_\mu$. In calculating fluxes from ordinary (non-prompt) sources, we again use the same model to describe π and K production and choose a value of 30 cm. for the absorption length of the dump.

Our calculations agree with the BEBC result that prompt sources of neutrinos dominate over π and K decays at 15 mr. A detector for prompt neutrinos should therefore sit away from 0 mr. However, in choosing an angle to look at, we must consider that as the angle becomes larger the average momentum of the neutrino becomes smaller. To observe a high flux of high energy prompt neutrinos, we have chosen the minimum angle subtended by our neutrino detector to be 10 mr. The maximum angle is largely dictated by shielding requirements and reasonable detector size. At 150 ft from the target, a 6-ft fiducial radius subtends 40 mr. The size and placement of the proposed neutrino detector is illustrated in Fig. 1. The calculated number of events expected in the detector for neutrinos originating from the various sources is shown in Fig. 2 as a function of the neutrino energy.

The decay of a massive object to a $\mu\nu$ pair implies a large opening angle. Since the neutrino detector is limited to relatively small forward angles, the muon detector should extend to as large an angle as possible. We have chosen an angle of $\sim$ 100 mr and a placement of $\sim$ 50 ft from the target as shown in Fig. 1. The minimum angle subtended is dictated by the rates at which we can run. Based on our Monte Carlo calculations of muon singles rates (which include all the above sources of $\mu\nu$ plus the observed dimuon production of Pilcher et al[5]), we can survive 10^{13} protons on target with θ_{min} = 30 mr and 10^{12} protons on target with θ_{min} = 20 mr. With θ_{min} = 20 mr, the acceptance for a muon with $P_\mu > 10$ GeV given an observed ν event with $P_\nu > 10$ GeV is $\sim$ 20% for charmed sources.

Measurement of the Reaction, $\nu_e(\bar{\nu}_e)+e^- \rightarrow \nu_e(\bar{\nu}_e)+e^-$

As remarked earlier, the production of neutrinos within the dump is expected to produce approximately equal fluxes of ν_μ, $\bar{\nu}_\mu$, ν_e, and $\bar{\nu}_e$. Consequently, this experiment represents an excellent opportunity to study for the first time the interactions of high energy electron neutrinos in general, and the elastic scattering reaction $\nu_e(\bar{\nu}_e)+e^- \rightarrow \nu_e(\bar{\nu}_e)+e^-$, in particular.

Measurement of both $\nu_e(\bar{\nu}_e)e$ elastic scattering and $\nu_\mu(\bar{\nu}_\mu)e$ elastic scattering provide a crucial test for any proposed theory of weak interactions since there are no uncertainties introduced due to any lack in our understanding of hadronic structure. The $\nu_e(\bar{\nu}_e)e$ elastic scattering cross section contains contributions from both neutral and charged current terms and so provides a measure of their interference. This information is not obtainable through the study of $\nu_\mu e$ elastic scattering since this reaction proceeds exclusively via the neutral current interaction.

The only measurement of $\bar{\nu}_e e$ elastic scattering comes from the Savannah River reactor using very low energy (1-8 MeV) antineutrinos.[6] They measure a cross section,

$$\sigma(\bar{\nu}_e + e^- \rightarrow \bar{\nu}_e + e^-) = (5.7 \pm 0.12) \times 10^{-42} E_\nu \ \mathrm{cm}^2/\mathrm{GeV} .$$

This result is consistent both with a pure V-A charged current or with a combination of charged and neutral currents with the Weinberg angle given by $\sin^2\theta_w = 0.29 \pm 0.05$. In the Weinberg-Salam model with $\sin^2\theta_w = 1/4$, the ratio of the charged plus neutral current to the purely V-A charged current cross section is given by,

$$\frac{\sigma(\nu_e e)_{WS}}{\sigma(\nu_e e)_{V-A}} = \frac{7}{12}$$

and

$$\frac{\sigma(\bar{\nu}_e e)_{WS}}{\sigma(\bar{\nu}_e e)_{V-A}} = \frac{3}{4} .$$

Clearly the $\nu_e e$ elastic scattering reaction provides better discrimination between the Weinberg-Salam and V-A hypotheses than does the $\bar{\nu}_e e$ elastic scattering. There have been no measurements of $\nu_e e$ elastic scattering at this time.

At this time there exist measurements of the elastic scattering reaction $\nu_\mu + e^- \rightarrow \nu_\mu + e^-$ both from Fermilab[7] and CERN.[8,9] The Columbia-Brookhaven experiment at Fermilab measures,

$$\sigma(\nu_\mu + e^- \rightarrow \nu_\mu + e^-) = (1.8 \pm 0.8) \times 10^{-42} E_\nu \ \mathrm{cm}^2/\mathrm{GeV} .$$

This result gives two possible solutions for the Weinberg angle, either $\sin^2\theta_w = 0.20^{+0.16}_{-0.08}$ or $\sin^2\theta_w = 0.57^{+0.7}_{-0.17}$. There is no such ambiguity in the determination of the Weinberg angle through the measurement of $\nu_e(\bar{\nu}_e)e$ elastic scattering. In Fig. 3 we display the values of the various cross section as a function of the Weinberg angle. Figure 3 shows explicitly that for values of $\sin^2\theta_w$ in the range of $0.2 \leq \sin^2\theta_w \leq 0.3$:

1) $\nu_e + e \rightarrow \nu_e + e$ gives better discrimination between the Weinberg-Salam and V-A hypotheses than does the reaction $\bar{\nu}_e + e \rightarrow \bar{\nu}_e + e$.

2) The $\nu_e(\bar{\nu}_e)$ elastic scattering is a stronger function of $\sin^2\theta_w$ than the $\nu_\mu(\bar{\nu}_\mu)$ elastic scattering and so gives a more precise measure of the Weinberg angle.

3) The cross sections for electron neutrinos are substantially higher than for muon neutrinos. For $\sin^2\theta_w$ = 0.25,

$$\frac{\sigma(\nu_e e \rightarrow \nu_e e)}{\sigma(\nu_\mu e \rightarrow \nu_\mu e)} = 7 \ ; \quad \frac{\sigma(\bar{\nu}_e e \rightarrow \bar{\nu}_e e)}{\sigma(\bar{\nu}_\mu e \rightarrow \bar{\nu}_\mu e)} = 3 \ .$$

We propose to build a detector to measure the $\nu_e(\bar{\nu}_e)e$ elastic scattering cross section. A measurement of the scattered electron direction with an accuracy of $\pm$ 1 mr allows a determination of the $y(=E_e/E_\nu)$ dependence of the reaction with a resolution of $\pm$ 0.1 in y. Since it is hard to imagine a detector which could distinguish between the ν_e's and $\bar{\nu}_e$'s which are expected in equal numbers, the y distribution will have a shape given by:

$$\frac{dN(\nu_e + \bar{\nu}_e)}{dy} \propto 1 + (1-y)^2 \ ,$$

independent of the Weinberg angle. This shape is given as long as the weak interaction Lagrangian contains only V and

A terms. Any deviation from this shape would be indicative of the presence of S, P, or T terms in the Lagrangian. As already stated, a measurement of the total cross section provides an accurate determination of $\sin^2\theta_w$. For $\sin^2\theta_w$ = 1/4, a 15% measure of $\sigma(\nu_e e \rightarrow \nu_e e)$ yields a 10% measure of $\sin^2\theta_w$.

Needless to say, a detector capable of measuring $\nu_e(\bar{\nu}_e)e$ elastic scattering is equally well suited to measuring $\nu_\mu e$ elastic scattering if run in a 'non-dump' mode. We estimate for normal wideband beam running with a flux equal to that existing at the Fermilab bubble chamber, an event rate for $\nu_\mu + e \rightarrow \nu_\mu + e$ of one event per 10^{16} protons on target.

A detector which could perform the functions described above would consist of a large quantity of acrylic scintillator interspersed with high resolution (σ = 0.25 mm) drift chambers. The scintillator serves both as production target and as the medium for electron shower development. The drift chambers are spaced so as to optimize the probability of measuring the electron direction before it starts to shower without sacrificing the lever arm needed to measure this direction accurately. The preferred spacing appears to us to be somewhere between 20 cm and 25 cm.

We have calculated the rates which we expect to observe in such a detector as well as rates due to the main sources of background. The results are shown in Fig. 4 as a function of the variable $E_e\theta_e^2$ which for the elastic scattering of neutrinos off electrons is kinematically constrained to be less than $2m_e$. The results are generated for 10^{19} proton-dump interactions assuming a 500-ton detector which accepts neutrinos in the range 10 mr to 40 mr and can detect electrons with energies greater than 2 GeV. The source of electron neutrinos is assumed to be charmed particles while the sources of muon neutrinos are both charmed particles, and pions and kaons which decay before being absorbed in the dump. The rate calculated for $\sin^2\theta_w = 1/4$ is approximately 300 $\nu_e(\bar{\nu}_e)+e \rightarrow \nu_e(\bar{\nu}_e)+e$ events per 10^{19} interacting protons. The major backgrounds are expected to be muon neutrino-electron elastic scattering and the inverse β decay reactions. The $\nu_\mu(\bar{\nu}_\mu)e$ reaction is suppressed by a factor of five relative to $\nu_e(\bar{\nu}_e)e$ for $\sin^2\theta_w = 1/4$. However, since there are alternative sources of muon neutrinos, the total suppression we expect in the detector becomes a factor of 3.

The contributions from $\bar{\nu}_e p \rightarrow e^+ n$ and $\nu_e n \rightarrow e^- p$ have been calculated assuming the cross section at $\theta = 0$ is given by:

$$\frac{d\sigma}{dQ^2}(\theta=0) = \frac{G^2}{\pi}\left[\frac{F_V^{\,2}+F_A^{\,2}}{2}\right],$$

where,

$$F_V(0) = 1 \text{ and } F_A(0) = 1.23.$$

The quasi-elastic reactions in carbon are suppressed at low momentum transfer by the Pauli principle. We have used a suppression factor of,

$$s = 1.5\left(\frac{P}{0.5\text{ GeV}}\right) - 0.5\left(\frac{P}{0.5\text{ GeV}}\right)^2,$$

where P is the momentum of the final state nucleon. The average effect of the suppression in the region where these events constitute a background is to reduce this background by a factor of 4. Based on the observations of the Columbia-Brookhaven collaboration, see Fig. 5, of the $\nu_\mu e$ reaction, we expect the contributions from processes such as $\nu N \to \nu N\pi^o$, followed by conversion of one of the γ rays to be inconsequential. Figure 5c shows the distribution of converted $\gamma \to e^+e^-$ events as measured in the Fermilab bubble chamber. The events represent a small background to the $\nu_\mu e^-$ elastic scattering and would represent a background five times smaller to the $\nu_e(\bar{\nu}_e)e$ reaction. Additional rejection of converted γ rays is possible by measuring the pulse height in the last 2 cm of scintillator directly before each chamber.

To summarize, for a run of 10^{19} interacting protons, we expect $\sim$ 300 $\nu_e(\bar{\nu}_e)e$ elastic scattering events plus $\sim$ 200 more background events mimicking this reaction.

The crucial factor which constrains the design of the detector is the need to measure the electron direction accurately. Measuring the electron accurately implies a large distance between drift chambers. However, making the distance too large becomes self-defeating for two reasons: 1) For spacings much greater than 30 cm, the contribution to the angular resolution from multiple scattering starts to dominate the contribution from chamber spatial resolution, and 2) for spacings much greater than 25 cm, an unacceptably large fraction of the electrons start to shower before their direction is measured.

We have calculated the resolution of the detector assuming we can measure the electron position at two different points to $\pm$ 0.25 mm. Figure 6 shows the measured $E\theta^2$ distribution with 20 cm chamber spacing as compared to the distribution we would see with infinite angular resolution. It turns out that the resolution in angle ($\sim \pm$ 1 mr) is very weakly dependent upon the chamber spacing because of the effects of multiple scattering. In Table I, we list for a sample of experiments completed or proposed to date, which measure νe elastic scattering, the angular resolution achieved or expected. The first four entries have been achieved; the final entries are expected.

We have investigated the effect of electron showering as it relates to the determination of the optimum chamber spacing. We have simulated the initial stages of the electron shower development and display the results in Fig. 7. Figure 7a shows the distribution in the spread of the electron shower at the second chamber for a 20 cm chamber spacing (so the average electron travels 30 cm before reaching the chamber). The electrons which reach the second chamber without having initiated a shower are entered at less than zero on the plot. We see that approximately 50% of the time a measurement can be made before showering starts. Figure 7b shows the results for 30 cm spacing. The effect of increasing the spacing is to greatly degrade our ability to measure the scattered electrons. While our ability to measure the direction of the electron sufficiently well for a meaningful determination of y is seriously hampered in approximately half the events, we still expect to be able to achieve a resolution of $\leqslant$ 7 mr on all events even in the presence of showers. This is because the low z (high critical energy) of scintillator tends to limit the lateral spreading of the showers. As in the case of the γ conversions, we will be able to separate the well measured from not-so-well measured events by observing the pulse in the last 2 cm of scintillator preceding each chamber. All events can be used for a determination of the total cross section while only the well measured ones would be used to determine the y dependence.

Based on the above considerations, we envision a detector along the lines of that shown in Fig. 8. The volume of scintillator is 14 ft x 14 ft x 70 ft with an x-y drift chamber pair every 20 cm of scintillator.

Table 1

Experiment	Reference	σ(mr)
Gargamelle	9	13
Aachen-Padova	8	17
Columbia-BNL	7	5
WA18 Proposal	10	10
CERN Proposal	11	2.4
Fermilab Proposal	12	10

The Tau Neutrino

One of the most exciting recent developments in particle physics has been the discovery, by Perl et al, of a new charged lepton, the tau.[13] It was first discovered by observing $e^+e^- \rightarrow e^+\mu^-$ with no additional hadrons. All existing data have continued to come entirely from e^+e^- experiments. Measurements by PLUTO, DASP, DELCO and others have confirmed these events, above and below charmed particle threshold, measured the energy dependence of the production cross section, the decay electron momentum spectrum and found the semileptonic tau decays, $\tau \rightarrow \nu_\tau \pi$, $\tau \rightarrow \nu_\tau \rho$, $\tau \rightarrow \nu_\tau A$, etc.[14] The mass of the tau has been determined by measuring its production threshold and is 1.8 ± 0.02. The most likely spin assignment for the tau is 1/2, based on the threshold energy behavior of the production cross section. A study of the decay electron momentum spectrum indicates that it is consistent with a three body decay ($\tau \rightarrow e\bar{\nu}_e\nu_\tau$) and furthermore indicates that the coupling is most likely (V-A). DELCO has measured the Michel parameter to be $\rho = 0.83 \pm 0.19$. One can also set limits on the ν_τ mass based on the observed kinematics. The best limit at present is $M_{\nu_\tau} < 250$ MeV/c^2. The existence of a new lepton number, requiring the existence of a new neutrino, ν_τ, remains untested. τ coupling to ν_μ can be ruled out by limits on τ production in neutrino experiments. However one cannot exclude the possibility that the τ carries the same quantum number as the electron, since no significant high energy ν_e experiments have been performed.

We propose an experiment to demonstrate the existence of a new quantum number, the tau lepton number, by showing that neutrino induced tau production occurs only from neutrinos produced by tau decay. Once the existence of a neutrino with a lepton number different from a ν_e or ν_μ is demonstrated, we will study its interaction with matter. In particular, we hope to measure its coupling strength.

The tau can be produced in pp collisions in a variety of ways. The simplest is via the Drell-Yan process, pp → $\tau^+\tau^-$+x. However, this cross section is too small to be useful. With the observation of copious charmed particle production in hadronic interactions in SPS beam dump experiments, it is clear that taus will be more abundantly produced in the decay of heavy charmed particles. Event rates for neutrinos from prompt processes and decays impinging on the proposed detector for 10^{19} protons on target are given in Fig. 2. Here we have made a 10 GeV neutrino energy cut.

It is clear that although there is a large yield of ν_τ events, a very significant ν_μ background still exists. If we concentrate on the $\tau \to \mu\nu\nu$ decay of the taus produced in the detector, we can use the kinematical differences between ν_μ and ν_τ events to reduce this background.

We assume ν_μ events interact via the standard charged current interaction Lagrangian. ν_τ's are assumed to interact via the same Lagrangian (μ-τ universality) but care is taken to keep all the mass terms. We use the following laboratory cross section to model tau production:

$$\frac{d\sigma}{dq^2 d\nu} = \frac{G^2}{8ME^2\pi}\Big[2k'\cdot kW_1 + \frac{W_2}{M^2}(k'\cdot kp^2 - 2k'\cdot pk\cdot p)$$
$$+ \frac{2W_3}{M^2}(k'\cdot qk\cdot p - k'\cdot pk\cdot q) + \frac{W_4}{M^2}(k'\cdot kq^2 - 2k'\cdot qk\cdot q)$$
$$+ \frac{W_5}{M^2}(k'\cdot kp\cdot q - k'\cdot pk\cdot q - k'\cdot qk\cdot p)\Big] \quad .$$

where k' is the tau four vector, k is the incident neutrino four vector and p is the proton four vector. Two new form factors, W_4, W_5 (suppressed by m_μ/m_p factors in ν_μ interactions) may be important in ν_τ interactions. In what follows, we assume that they are zero. The resulting cross section energy dependence of ν_μ and ν_τ is shown in Fig. 9. The energy distribution of ν_μ and ν_τ events is shown in Fig. 10. The tau is modeled to decay via $\tau \rightarrow \mu\nu\nu_\tau$. Since the two neutrinos in the final state are not detected, we expect a large missing transverse momentum in these events, as well as a strong distortion of the observed x and y distribution. The visible y distribution for $\bar{\nu}_\tau$ reactions is particularly different from the distribution in $\bar{\nu}_\mu$ events. Below, we will use this to search for the existence of $\bar{\nu}_\tau$ events.

The details of x, y and $p_\perp$ missing distributions depend on the detector resolution. Here we make the following assumptions: 1) The detector measures $\Delta\theta_\mu \sim \pm 0.006$ and $\Delta P_\mu/P_\mu \sim \pm 0.1$ and $\Delta E_h/E_h \sim \pm 0.9/\sqrt{E_h}$, and $\Delta\theta_h \sim \pm 0.003 + 0.4/E_h$; i.e. we measure the hadron energy flow magnitude and direction and the muon momentum and angle. These resolutions are consistent with what has been previously achieved in large detectors and we expect to do better, but these achieved resolutions will be used in our present discussion. Figure 11 shows the missing transverse momentum distribution for ν_μ and ν_τ events with experimental resolution folded in.

If we cut events with $P_\perp$ missing < 1.2 GeV/c, a reduction of $\sim 10^{-2}$ can be achieved in ν_μ charged current events. This cut also reduces the ν_τ signal by a factor of 2. We should note that this reduction depends sensitively on the angular resolution of the hadron energy flow vector.

After this cut, we are left with 2.8×10^3 $\nu_\tau N \to \tau + x$ (with $\tau \to \mu\nu\nu$) and 1.8×10^4 ν_μ events. We can further reduce the background by the following consideration. $\tau^+ \to \mu^+\nu_\mu\bar{\nu}_\tau$, whereas $D^- \to K^o\mu^-\bar{\nu}_\mu$. It follows that if a $\bar{\nu}_\tau$ or a $\bar{\nu}_\mu$ interacts in the detector and produces a μ^+ in the final state, the parent particle will decay into a μ^+ for the $\bar{\nu}_\tau$ and a μ^- for the $\bar{\nu}_\mu$. A similar situation holds for ν_μ and ν_τ events. If the μ from this decay can be tagged and its sign measured, a further signal to noise reduction is possible.

We propose to tag the muon with the muon detector and measure its sign and four momentum. If we accept only like sign events (tagged muon and μ from neutrino interaction) and make minimum cuts of $P_{\mu} > 2.0$ GeV and $E_h > 2.0$ GeV on neutrino events, we find 540 ν_{τ}, 730 ν_{μ} and $\sim$ 200 $\bar{\nu}_{\tau}$, 300 $\bar{\nu}_{\mu}$ events, where the background is now entirely from D decays. The signal to noise is $\sim$ 1 to 1. With this signal to noise level, the measured visible y distributions will give clear evidence for the existence of the $\bar{\nu}_{\tau}$ signal. Figure 12 shows the x, y distribution for the $\bar{\nu}_{\tau}$ and remaining $\bar{\nu}_{\mu}$ events.

The observation of an enhancement of events with large missing transverse momentum when a same sign muon is tagged, implies that the interacting neutrino has a quantum number different from the electron or the muon. If the tau neutrino carried electron lepton number, events with and without tagged muons would be equally likely to have taus in the final state, i.e.

$$\tau^- \to \mu^-(\bar{\nu}_{\mu})\nu_e \; ; \qquad \nu_e N \to \tau + x, \quad \tau \to \mu^- + \nu\nu$$

$$D^+ \to K^o e^+ \nu_e \; ; \qquad \nu_e N \to \tau + x, \quad \tau \to \mu^- + \nu\nu \; .$$

If we assume μ, e, τ universality, the ν_τ matrix element is identical to that for ν_μ's and ν_e's. However, form factors which enter multiplied by m_μ/m_p factors will now be in principle significant and may be observable in their effect on the visible x and y distributions. The sensitivity to these form factors depends on the F/D ratio and the statistics accumulated. We will however clearly be able to test for consistency with known form factors.

Since the tau is very massive, the approximate helicity conservation of ν_μ, ν_e charged current interactions does not hold and significant tau polarization effects may be expected at $Q^2 > 1$ $(GeV/c)^2$. Such effects are very important.

We do not presently propose to measure muon polarization but the detector as envisaged with minor modification can be expanded at a later date to allow such measurement if physics warrants this.

Because the hadron energies in these reactions are not high ($\sim$ 10-20 GeV) and the θ_H resolution critical, it is essential that the detector be designed for high sampling, high resolution calorimetry. The 500-ton acrylic scintillator-drift chamber detector has fine sampling and will be used to measure lower energy hadron events, while the 1-in. magnetized Fe plate detector will be used for higher energy $E_h \geq 20$ GeV events. The quoted energy resolution has been previously achieved for coarser sampling (2 in.) detectors and we should be able to do as well or better.

Muons and Neutrinos in Coincidence

Aside from its important role as a tagging device for the study of the tau neutrino, the proposed muon detector can be used for a wide variety of novel studies. By detecting neutrinos and muons in coincidence we can study the hadronic production of charmed mesons as well as the production of heavier states with new quantum numbers such as top and bottom.

The hadronic production and semileptonic decay of charmed particles should provide the major source of electron neutrinos for this experiment. It is thus interesting for this and other reasons to study the hadronic production of D mesons. We propose to do this by obtaining the invariant mass distribution for muons and neutrinos detected in a coincidence from the dump. As shown in Fig. 13, the invariant mass spectrum from the decays, $D \rightarrow k\mu\nu$ or $D \rightarrow K^{*}\mu\nu$, has a characteristic enhancement in the vicinity of 1 to 2 GeV/c^2.

This enhancement lies substantially higher in mass than the spectrum of uncorrelated μ,ν pairs from kaons and pions decaying before absorption in the dump, and our resolution should be adequate to maintain this separation. Hence a study of the experimental $\mu\nu$ invariant mass distribution will allow us to test the assumption that charmed meson decays form a major source of detected neutrinos from the beam dump. If the bulk of the neutrinos are produced by D meson decays, as expected, one can safely assume the number of electron neutrinos will equal the number of muon neutrinos. Thus we can determine our electron neutrino flux, by clean measurements of the rate for $\nu\mu$ induced events in the neutrino detector.

We have performed a Monte Carlo simulation of hadronic $D\bar{D}$ production and subsequent semileptonic decay using a variety of models. These simulations indicate that the geometrical acceptance for detecting a muon in coincidence with a neutrino with both particles having an energy of greater than 10 GeV is $\simeq$ 10%. Using our proposed neutrino detector tonnage and the assumption that 1 out of 400 protons produces a charmed meson pair, we should see about 1 usable $\mu\nu$ coincidence from D decays for every 10^{14} protons interacted.

With these momentum cuts and our geometry, we estimate a small contamination of the $\mu\nu$ invariant mass plot from uncorrelated decays of pions and kaons before absorption in the dump. In particular, we expect less than 10^{-7} false $\mu\nu$ coincidences per pulse of 10^{13} protons for $\mu\nu$ masses greater than 1 GeV/c^2 from these sources.

Lastly the muon detector with the neutrino detector in coincidence provides a novel way to search for the semi-leptonic decays of heavier mass objects with new quantum numbers such as bottom and top states. Monte Carlo calculations show that our $\mu\nu$ acceptance for a bottom particle (B) of mass 5 GeV/c^2 decaying via $B \rightarrow D\mu\bar{\nu}$ is comparable to the acceptance of $\mu\nu$ coincidence from D pairs.

Muon neutrino coincidences from B or T particles would populate the $M_{\mu\nu}$ distribution at still higher masses than coincidences from D meson decays, offering still smaller backgrounds from conventional sources.

Miscellaneous

Using the wide variety of detectors employed in this experiment, we may be able to investigate more speculative phenomena including the possible existence of axions, charged Higgs particles, new intermediate mass gauge bosons, and neutral heavy leptons. Axions having the property of high penetration through ordinary matter could be found by their interactions in the neutrino detector. These interactions would be differentiated from ordinary ν interactions by an absence of $P_{\perp}$ imbalance in the hadronic energy flow. The presence of charged Higgs particles ($H^{\pm}$) decaying via $H^{\pm} \rightarrow \mu^{\pm}\nu$ would be observed as a bump in the $\mu\nu$ invariant mass distribution, as would the presence of new charged gauge bosons of intermediate mass decaying via $W_2^{\pm} \rightarrow \mu^{\pm}\nu$. Finally a signature for a neutral muonlike heavy lepton would be a bump in the tri-lepton distribution: $M^{o} \rightarrow \mu^{-}\mu^{+}\nu$.

Detectors

This section will describe the overall dimensions of the muon tagging detector, neutrino detector and electron detector. More detailed descriptions of the detector's performance and design consideration are discussed in previous sections.

Muon Tagging Detector

The muon tagging detector will measure the angle and momentum of muons produced through the decay of parent particles in the dump. This device consists of four sets of three multistep avalanche planes.

Two sets will be placed before a 10 ft long, 7 ft radius magnetized iron torroid. This will be followed by the remaining two sets.

Multistep avalanche chambers offer the ability to store the trajectory information in a drift space until a trigger arrives from the neutrino detector. Our chambers will have a spatial resolution of approximately 2 mm, and should be as fast as possible in order to withstand the high singles rates near the dump.

Neutrino Detector

The neutrino detector is a magnetized iron calorimeter. The detector will be split into two halves with each half consisting of four units (Fig. 1). All units contain twenty, 7-ft radius iron plates magnetized to approximately 20 kG.

We will use 1-in. thick plates in the first three sections and 3-in. plates in the fourth. The area between the plates will be covered by 12-in. wide x 1-in. thick scintillation counters. Three planes of x, y, u drift tubes follow each unit. The scintillation counters will be viewed at both ends by phototubes through wave shifter bars and each scintillation plane will also be summed with wave shifter bars on two sides. The drift tubes will be approximately 30-cm wide, 2-cm thick and 14-ft long. The sense wire-field wire spacing will be ~ 3.0 cm.

Electron Detector

The electron detector consists of two sections, each 14 ft x 14 ft x 35 ft followed by a torroidal calorimeter section as in Fig. 1. The arrangement of scintillator and drift tube chambers is shown in Fig. 8. Positioning the chambers every 20 cm gives a system containing 84000/d wires where d is the wire spacing in centimeters. We hope to use d $\approx$ 3 cm. The acrylic scintillator sections are 15 cm x 20 cm x 14 ft each and are viewed by phototubes on each end. Pulse height in the last 2 cm of scintillator will be measured separately so that the presence of e^+e^- pairs entering the chambers can be detected.

We note that apart from the multistep avalanche chambers, all the detectors we envision using are well known, easily mass produced, and have been used successfully in other large experiments.

Summary

The production of prompt neutrinos within a beam dump presents the opportunity to measure processes involving electron neutrinos and tau neutrinos for the first time. Observation of the accompanying muon not only results in a tagging of the ν_τ induced interactions but also raises the possibility of identifying new heavy sources of muons and neutrinos. The study of both the $\nu_e(\bar{\nu}_e)e$ elastic scattering reaction and the interactions of the tau neutrino represent new fundamental tests of our understanding of weak interactions and so should be carried out. The detector described in this proposal combines sufficient discrimination against background with high enough interaction rates to allow a statistically meaningful measurement of these processes over a two-year period of time.

We acknowledge the contributions of A. Abashian and R. Orr to the planning and preparation of this proposal.

References

[1] P. Alibran et al, Phys. Lett. 74B, 134 (1978).
T. Hansl et al, Phys. Lett. 74B, 139 (1978).
P. Bossetti et al, Phys. Lett. 74B, 143 (1978).

[2] H. Wachsmuth, Proceedings of the Topical Conference on Neutrino Physics, Oxford (1978).

[3] M. Bourquin & J.-M. Gaillard, Nucl. Phys. B114, 334 (1976).

[4] Gaillard & Quigg; private communication.

[5] K.J. Anderson et al, Phys. Rev. Lett. 37, 799; 803 (1976).

[6] F. Reines et al, Phys. Rev. Lett. 37, 315 (1976).

[7] A.M. Cnops et al, Phys. Rev. Lett. 41, 357 (1978).

[8] H. Faissner et al, Phys. Rev. Lett. 41, 213 (1978).

[9] P. Alibran et al, Phys. Lett. 74B, 422 (1978).

[10] Aachen-CERN-Frascatti et al proposal, CERN/SPSC/75-59.

[11] CERN et al proposal CERN/SPSC/79-30.

[12] J. Walker et al, Fermilab proposal.

[13] Perl et al, Phys. Rev. Lett. 35, 1489 (1975).

[14] G.J. Feldman in Proceedings of the 19th International Conference on High Energy Physics, Tokyo (1978).

Fig. 1 Layout of the detector.

Fig. 2 Events expected in the detector per 10^{17} protons on target per 5 GeV.

Fig. 3 Total cross sections for neutrino-electron elastic scattering processes, in the W-S model, as function of $\sin^2\theta_W$.

Fig. 4 Rate calculation of the three major sources of single electrons in the electron detector. Rates are for 10^{19} interacting protons. The source of ν_e's is charmed particle production; the source of ν_μ's is both charmed particle and π/K production.

Fig. 5 Distribution in $E\theta^2$(MeV) for single electron events produced by muon neutrinos in the Fermilab bubble chamber.

Fig. 6 The dashed curve shows the expected smearing in the measured $E\theta^2$ distribution from the effects of chamber resolution, multiple scattering, and energy resolution.

Fig. 7 The expected spread in the electron shower at the second measuring chamber for chamber spacings of 20 cm and 30 cm. Entries at less than zero are events with no showering before the second chamber.

Fig. 8 The arrangement of scintillator and drift chambers in the electron detector.

Fig. 9 Energy dependence of cross section for ν_μ, ν_τ .

Fig. 10 Energy distribution of events for ν_μ, ν_τ .

Fig. 11 Missing transverse momentum for ν_μ, ν_τ events.

Fig. 12 Visible x and y distributions for $\bar{\nu}_\mu$, $\bar{\nu}_\tau$.

Fig. 13 Invariant mass distribution of accepted $\mu\nu$ pairs with resolutions described in text.

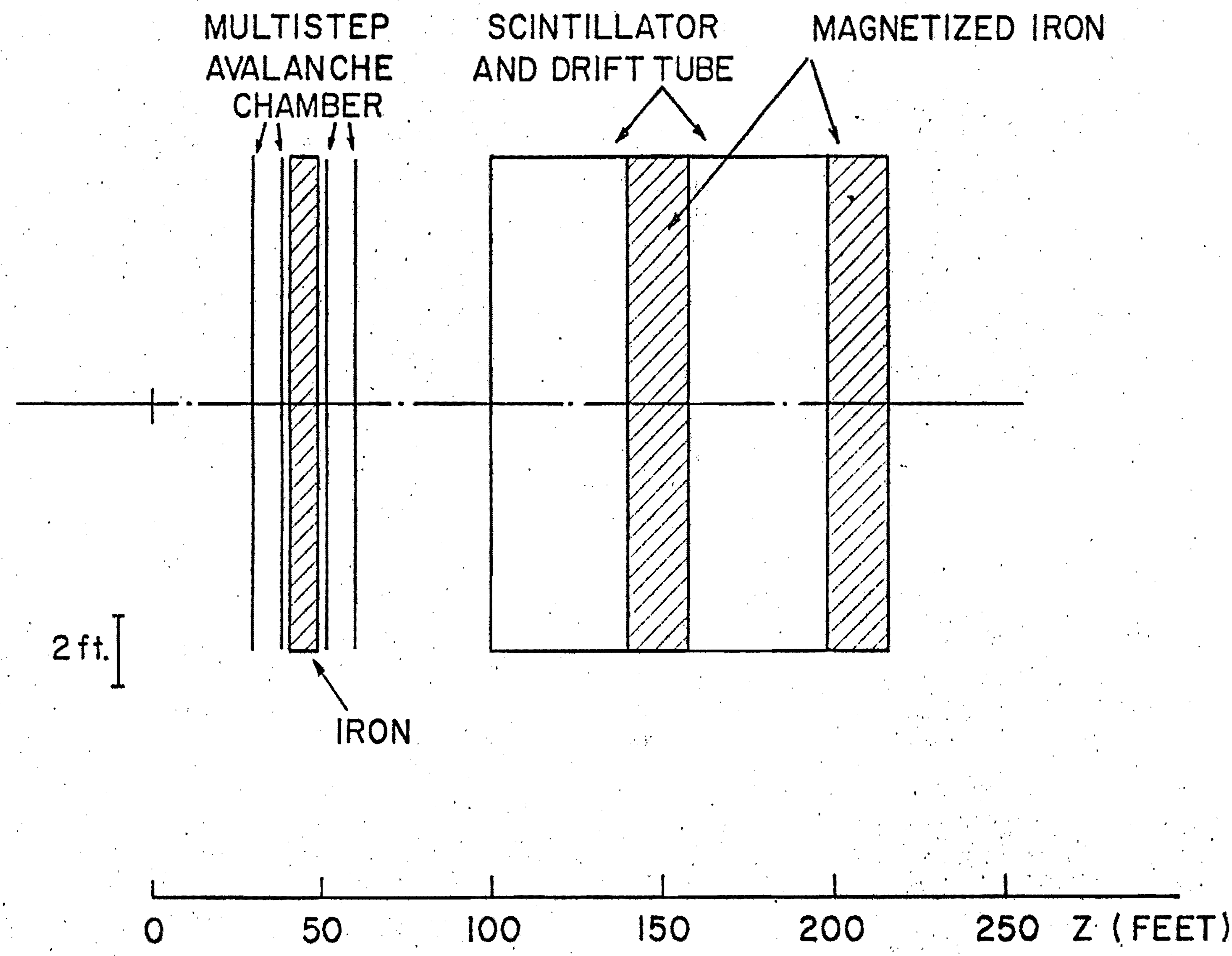
MULTISTEP AVALANCHE CHAMBER
SCINTILLATOR AND DRIFT TUBE
MAGNETIZED IRON
2 ft.
IRON
0
50
100
150
200
250
Z (FEET)

Fig. 1

Fig. 2

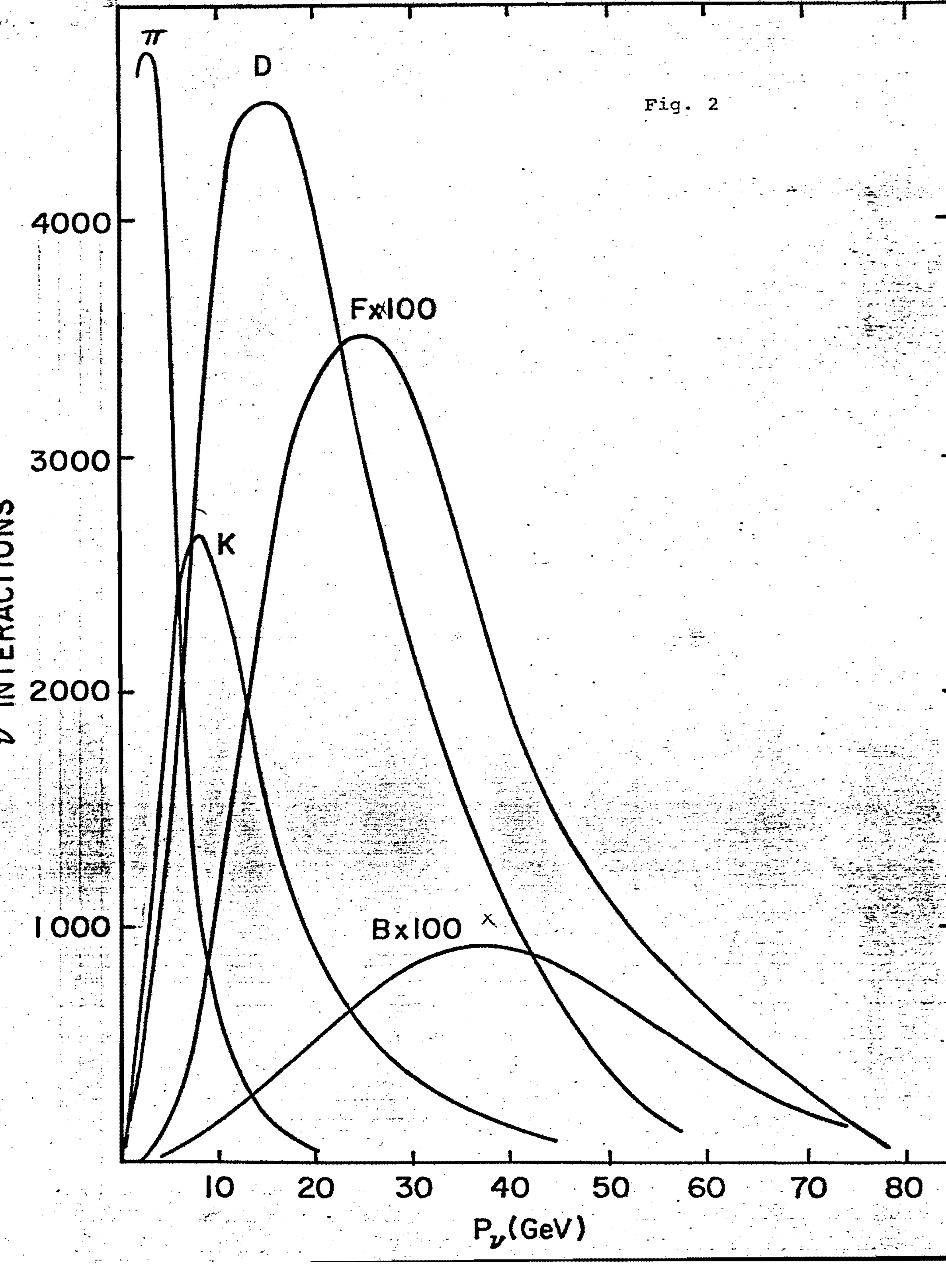

π
D
FxIOO
K
BxIOO
4000
3000
2000
1000
ν INTERACTIONS
10
20
30
40
50
60
70
80
P_ν(GeV)

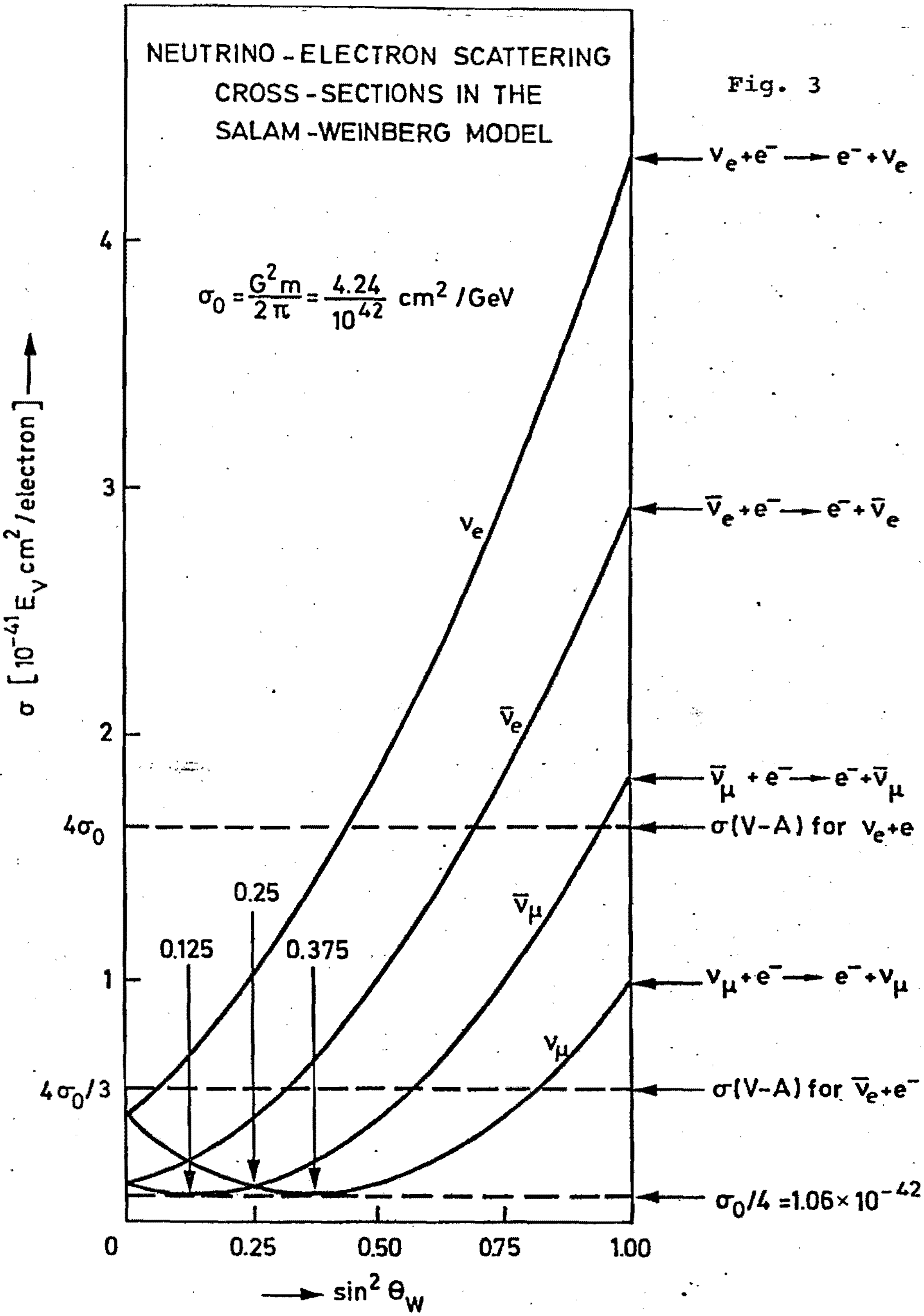
NEUTRINO - ELECTRON SCATTERING CROSS - SECTIONS IN THE SALAM - WEINBERG MODEL
$\sigma_0 = \frac{G^2 m}{2\pi} = \frac{4.24}{10^{42}}$ cm^2 /GeV
σ [10^{-41} E_ν cm^2 /electron]
$\nu_e + e^- \rightarrow e^- + \nu_e$
$\bar{\nu}_e + e^- \rightarrow e^- + \bar{\nu}_e$
$\bar{\nu}_\mu + e^- \rightarrow e^- + \bar{\nu}_\mu$
σ(V-A) for ν_e+e
$\nu_\mu + e^- \rightarrow e^- + \nu_\mu$
σ(V-A) for $\bar{\nu}_e + e^-$
$\sigma_0/4 = 1.06 \times 10^{-42}$
$4\sigma_0$
$4\sigma_0/3$
0.125
0.25
0.375
0
0.25
0.50
0.75
1.00
$\sin^2\theta_W$

Fig. 3

Fig. 4

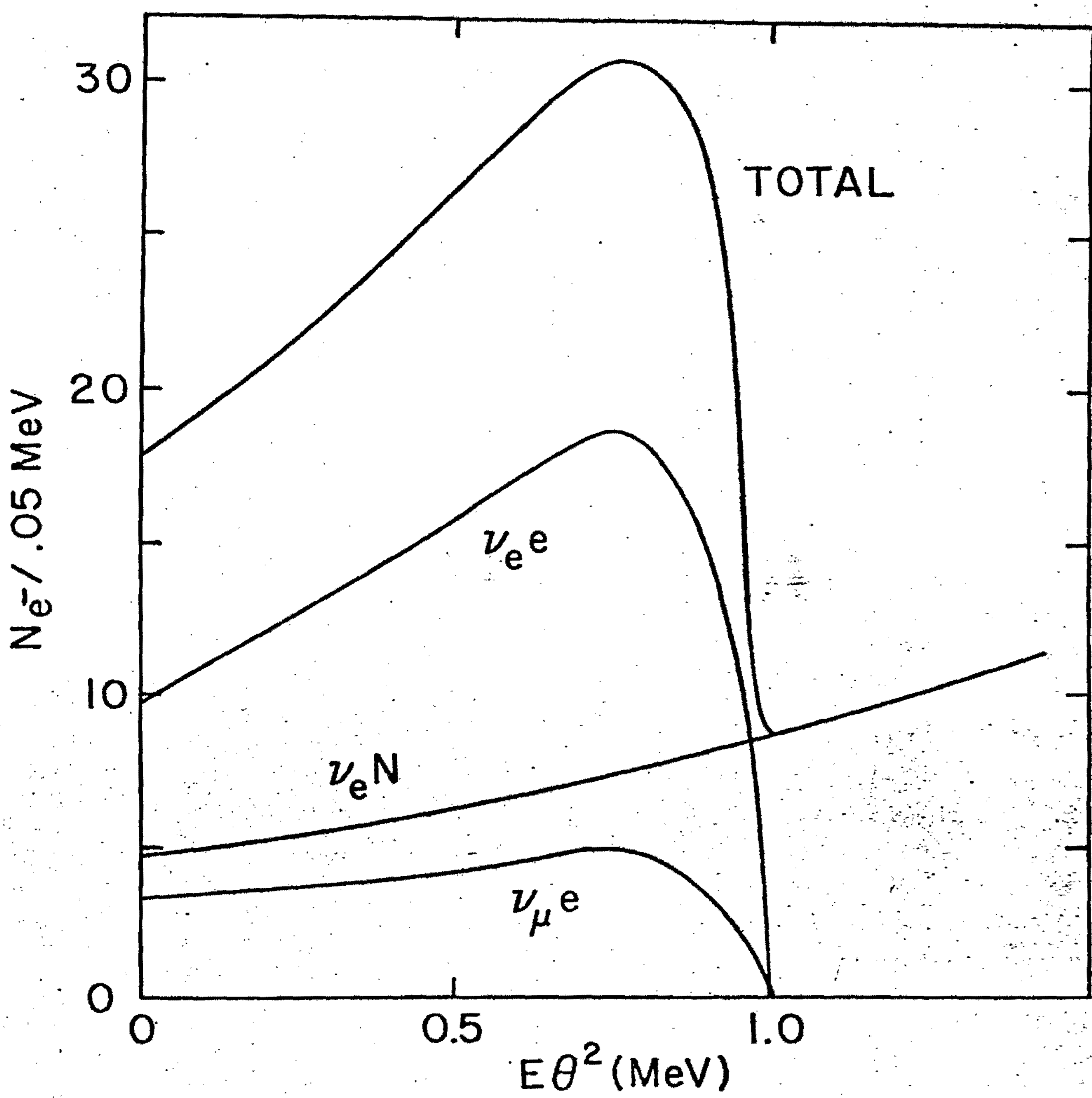

Fig. 5

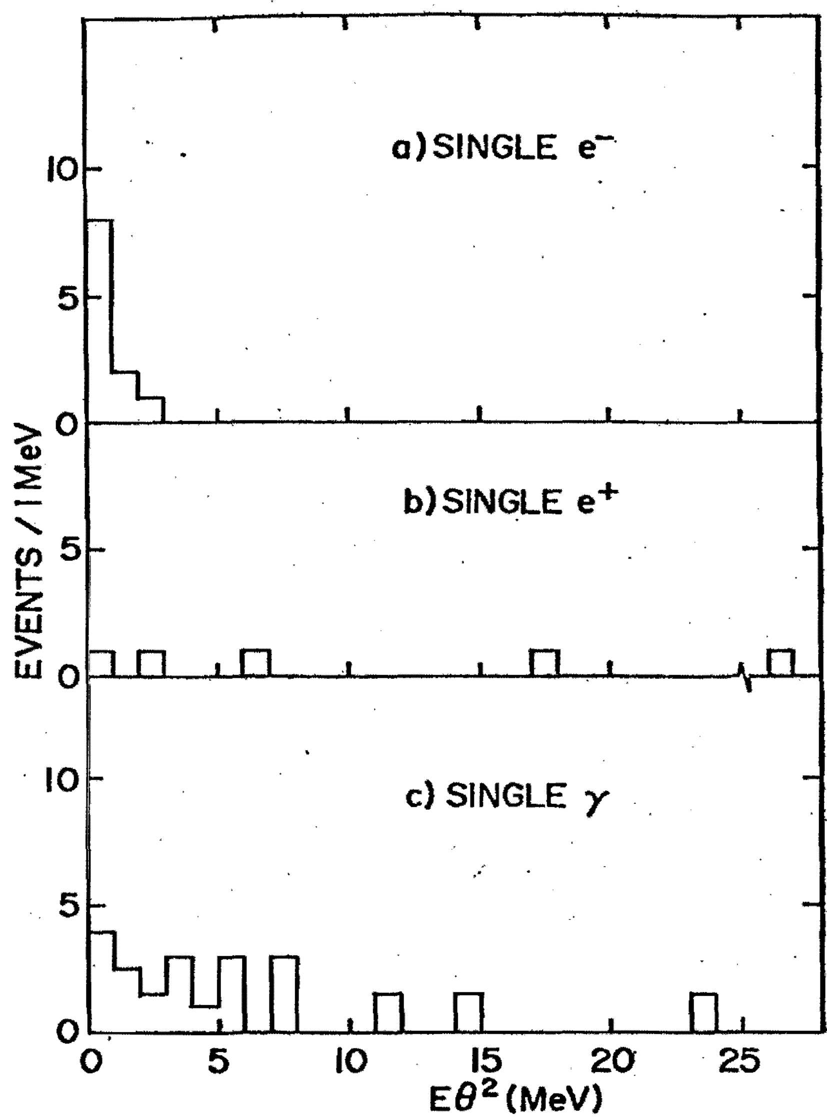

a) SINGLE e⁻
b) SINGLE e⁺
c) SINGLE γ
EVENTS / 1 MeV
0
5
10
0
5
0
5
10
0
5
10
15
20
25
Eθ² (MeV)

Fig. 6

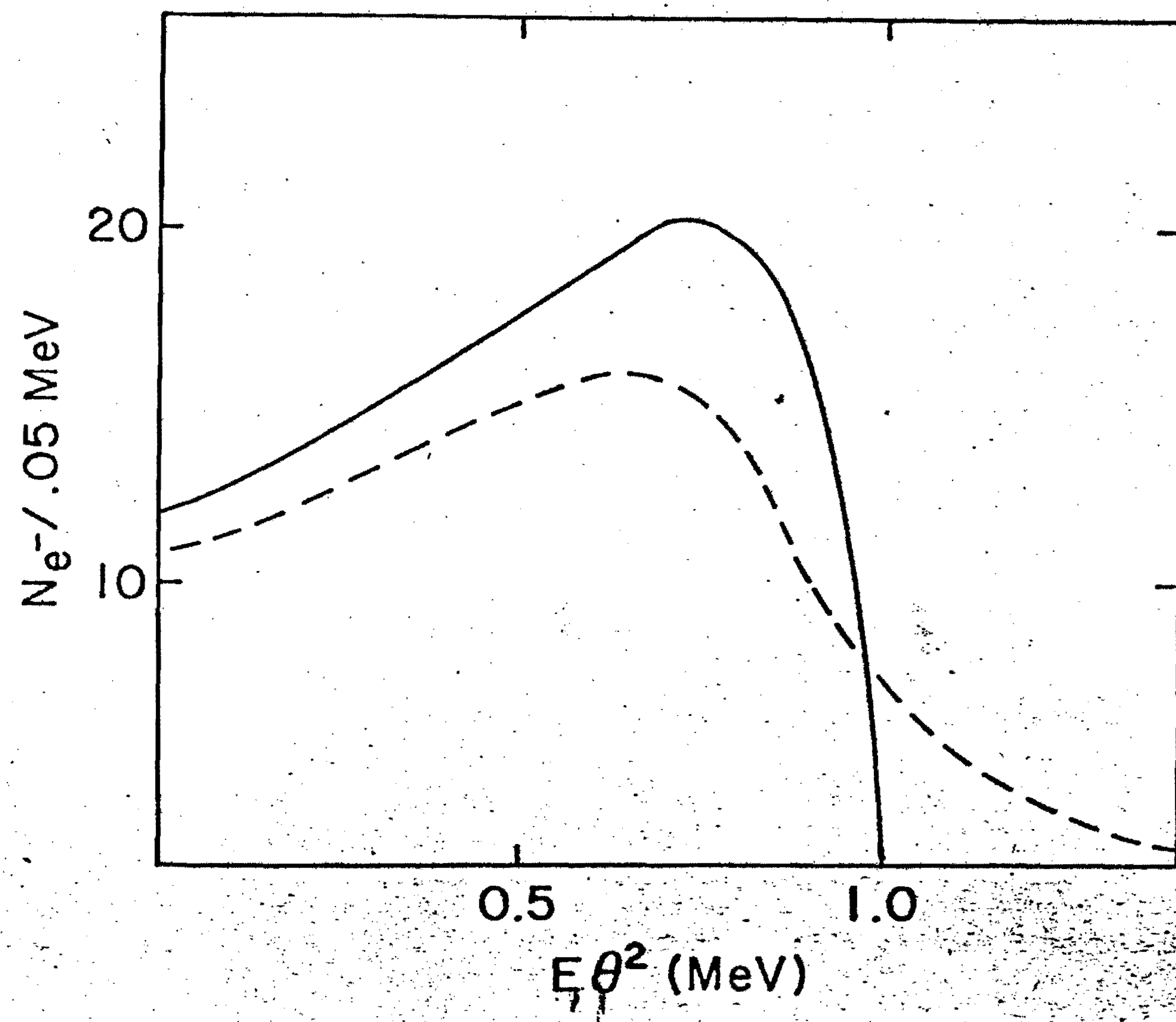

Fig. 7

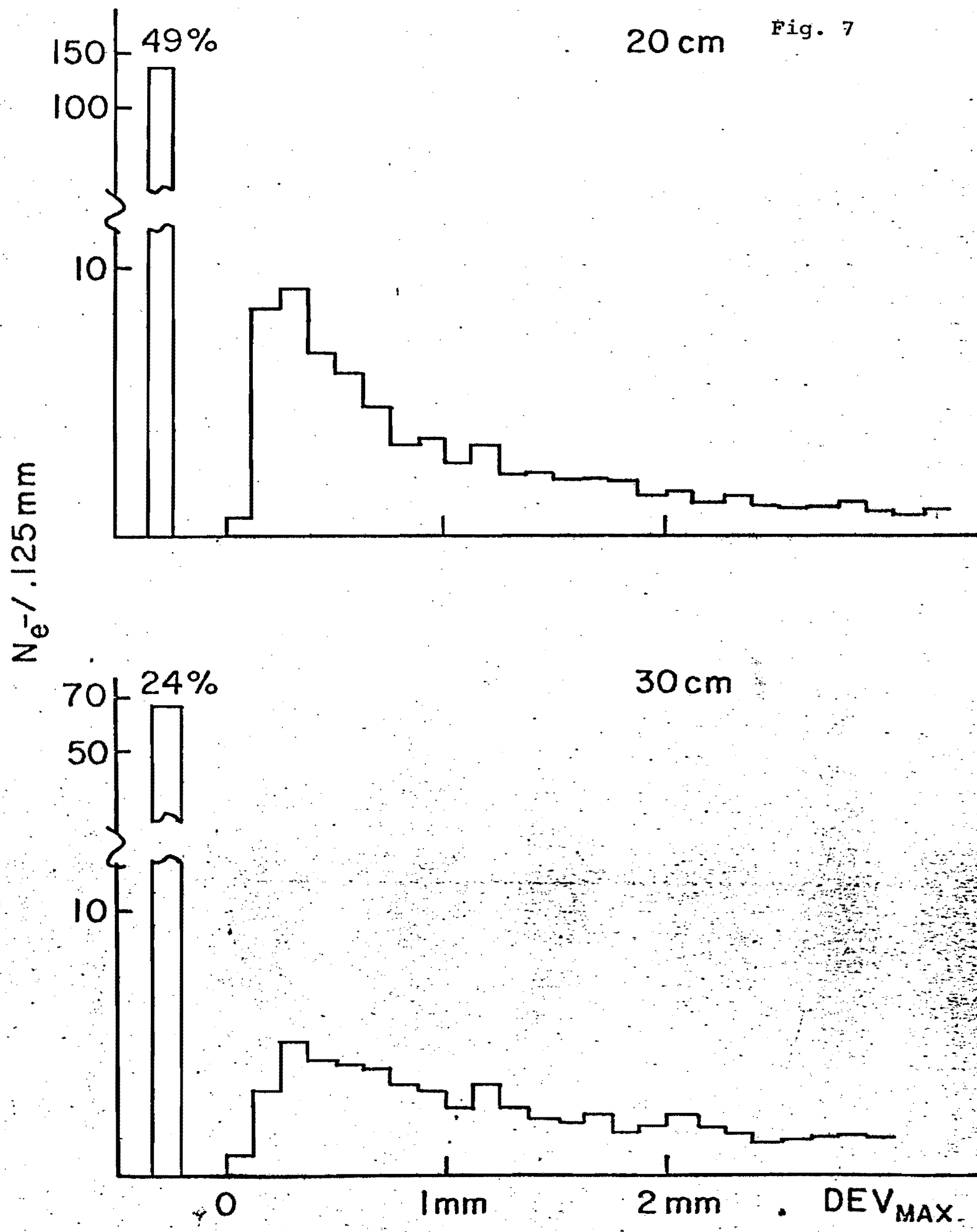

Fig. 8

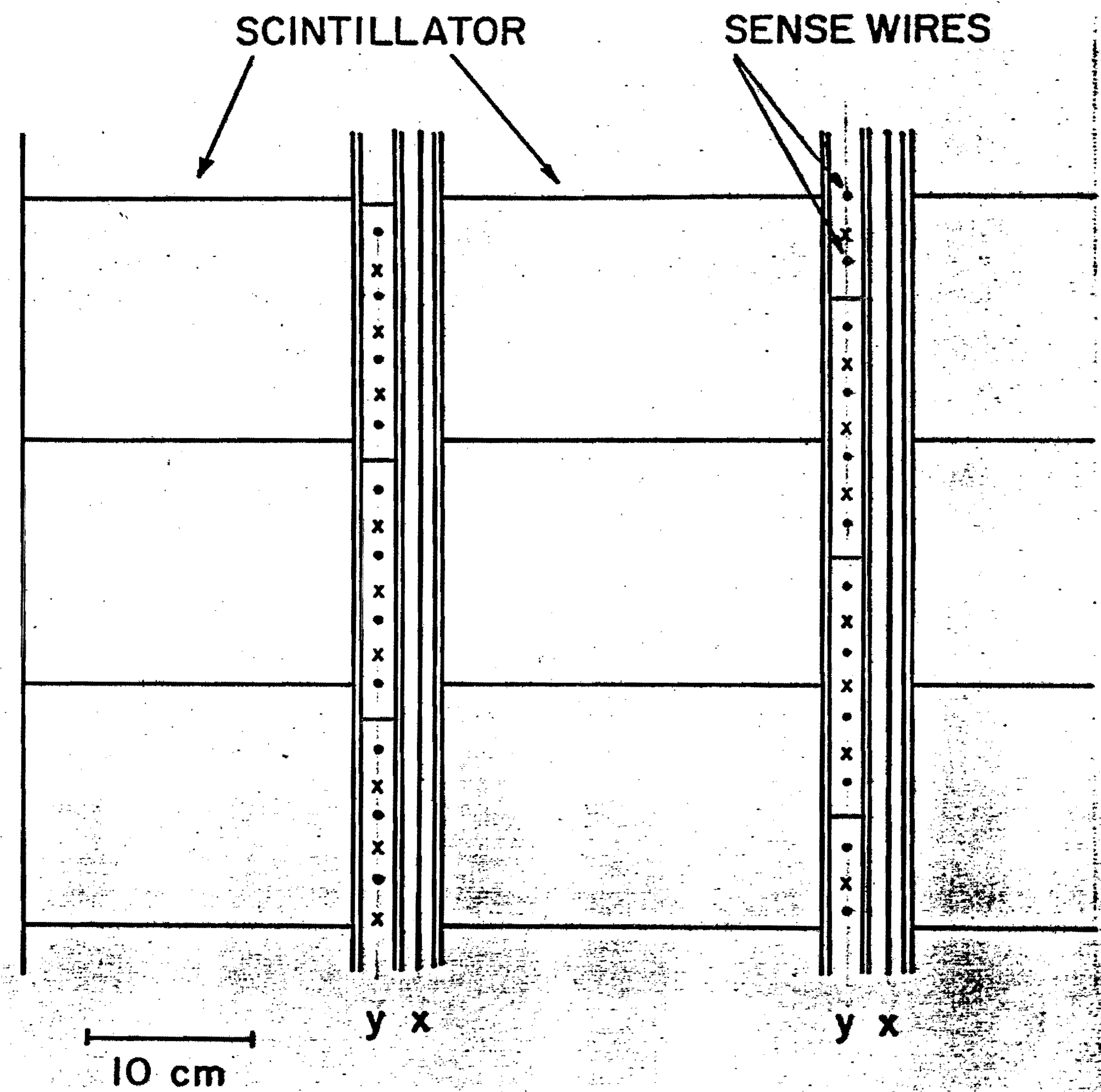

Fig. 9

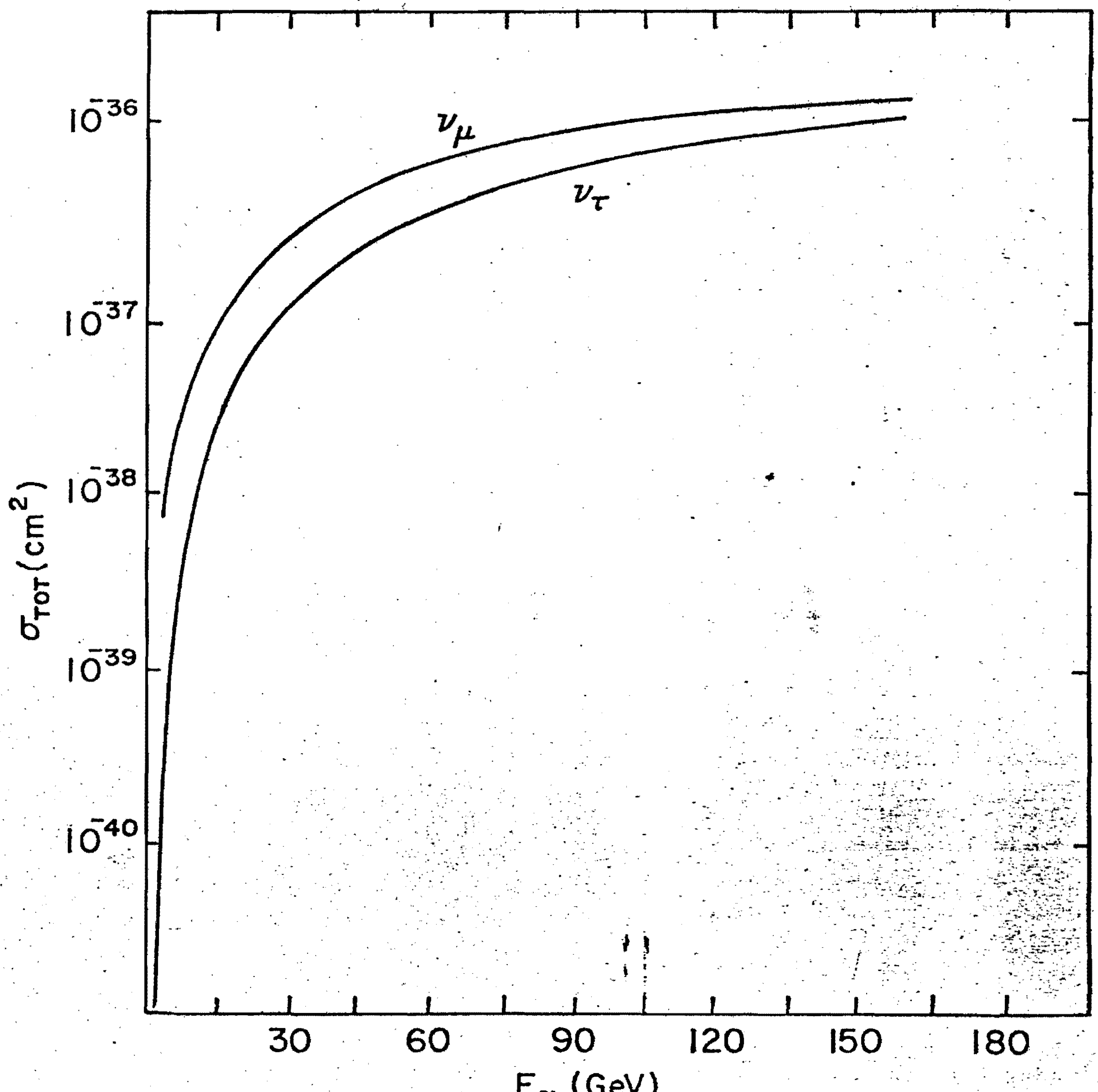

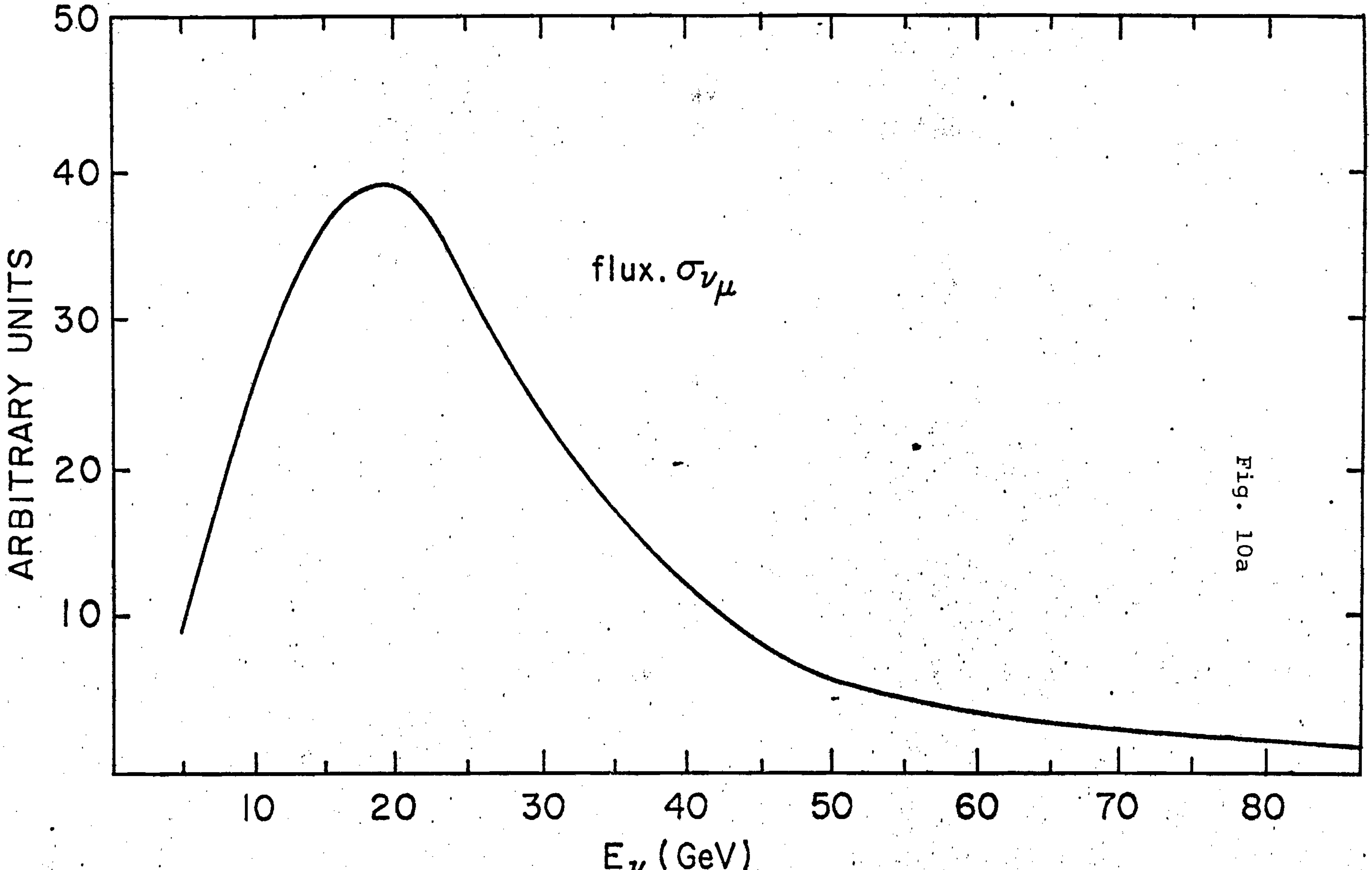

50
40
30
20
10
ARBITRARY UNITS
flux. σ_{ν_μ}
10
20
30
40
50
60
70
80
E_ν (GeV)

Fig. 10a

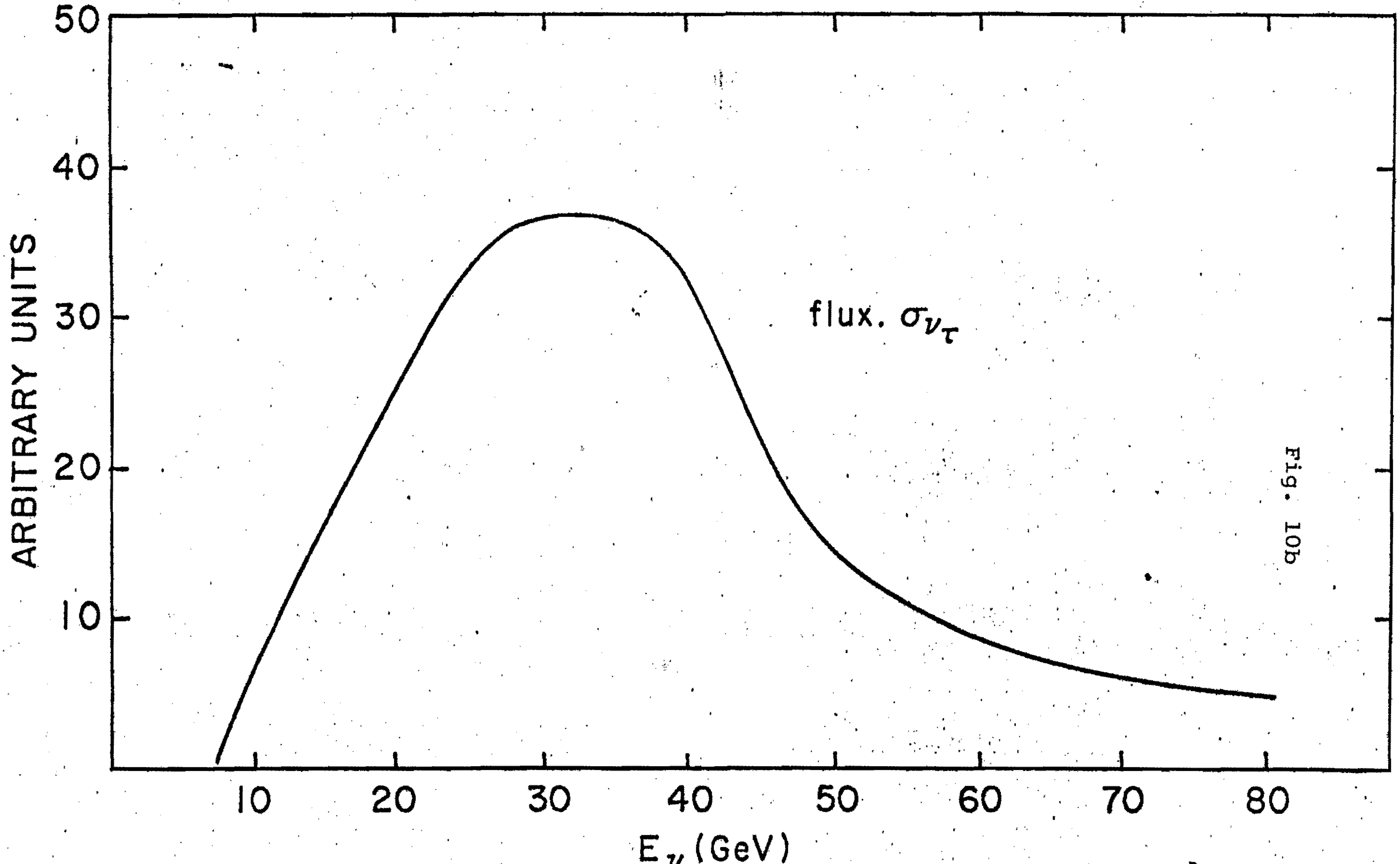

50
40
30
20
10
ARBITRARY UNITS
flux. σ_{ν_τ}
10
20
30
40
50
60
70
80
E_ν (GeV)

Fig. 10b

Fig. 11

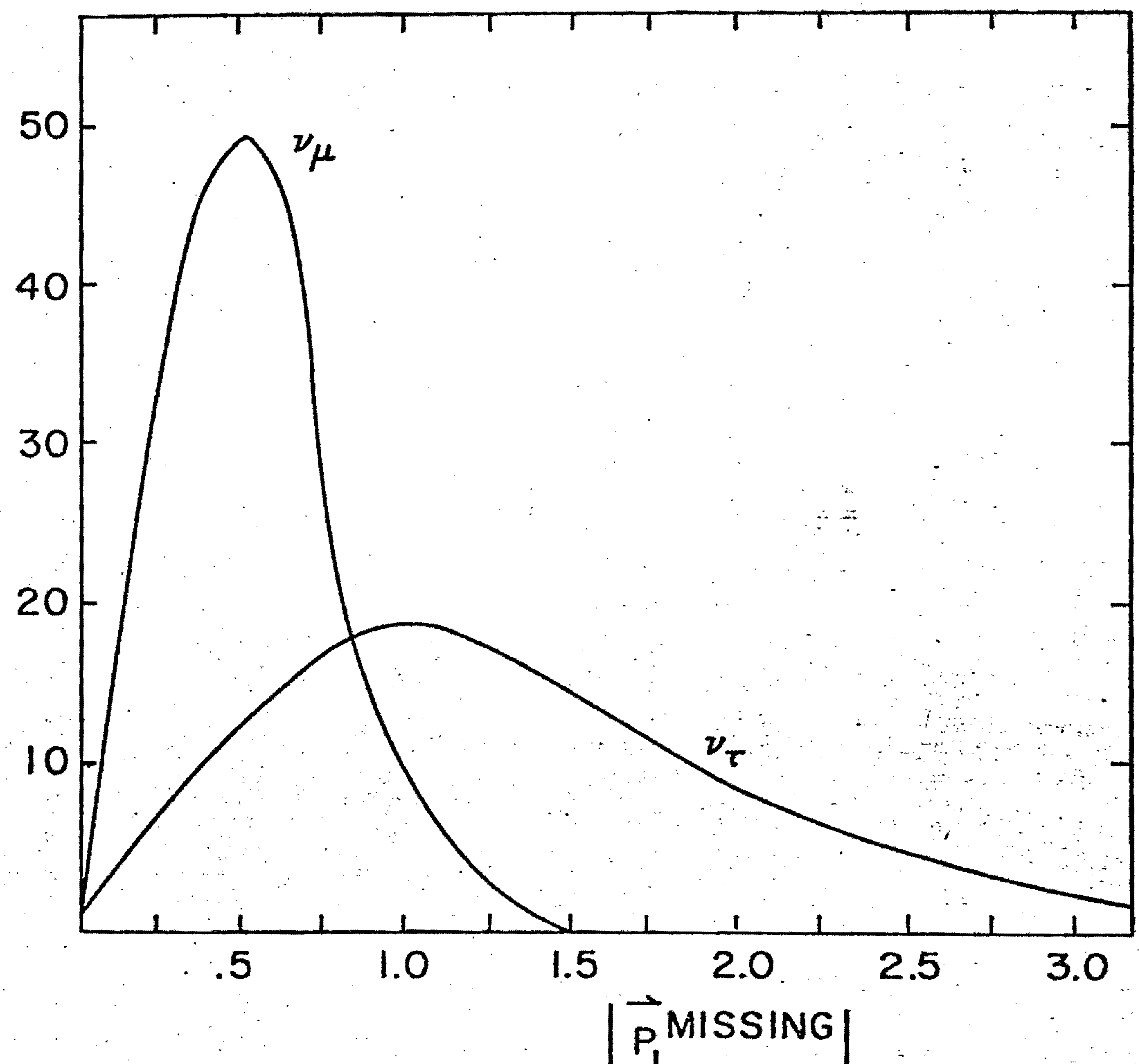

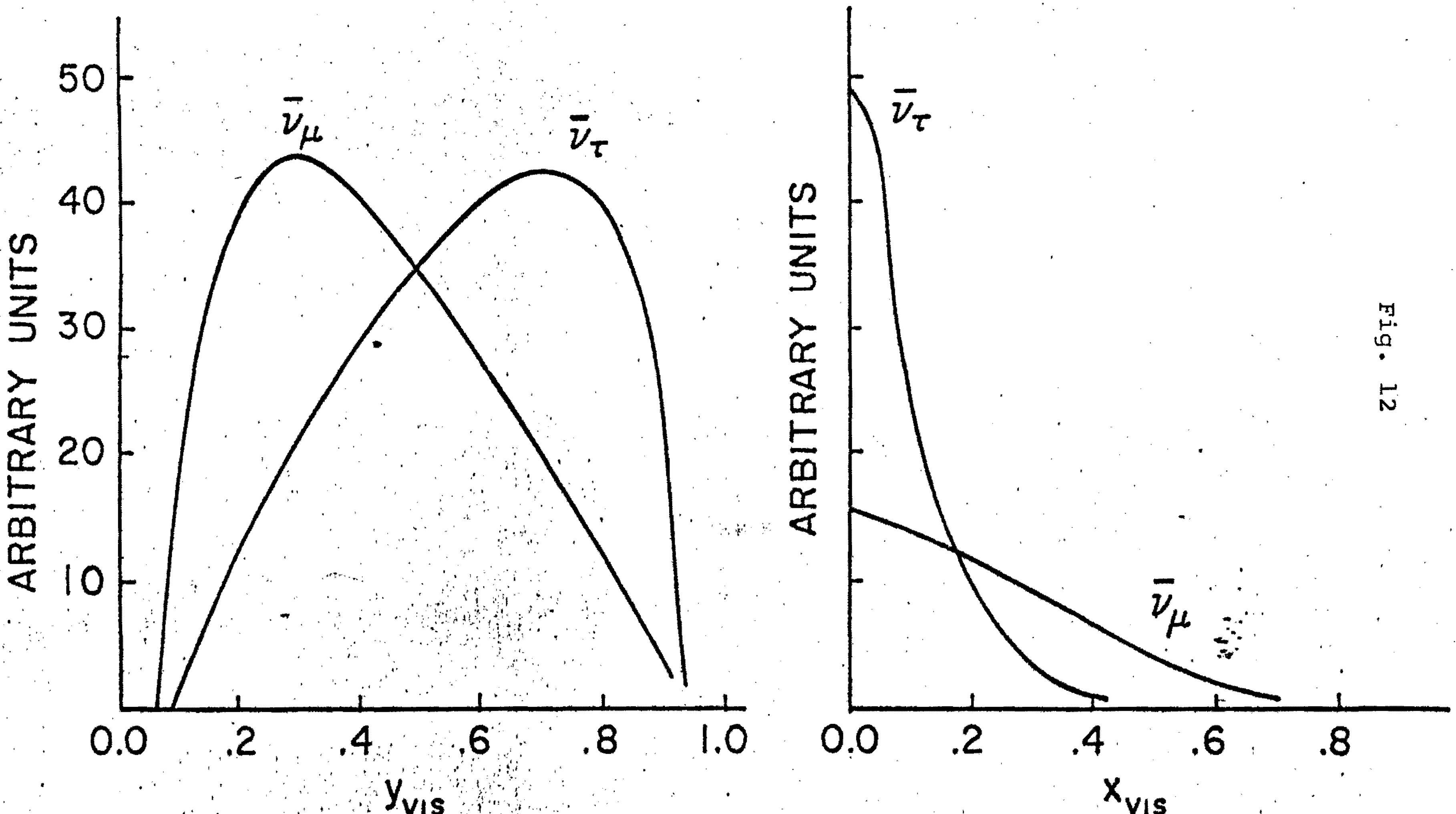

ARBITRARY UNITS
50
40
30
20
10
$\bar{\nu}_\mu$
$\bar{\nu}_\tau$
0.0
.2
.4
.6
.8
1.0
y_{VIS}
ARBITRARY UNITS
$\bar{\nu}_\tau$
$\bar{\nu}_\mu$
0.0
.2
.4
.6
.8
x_{VIS}

Fig. 12

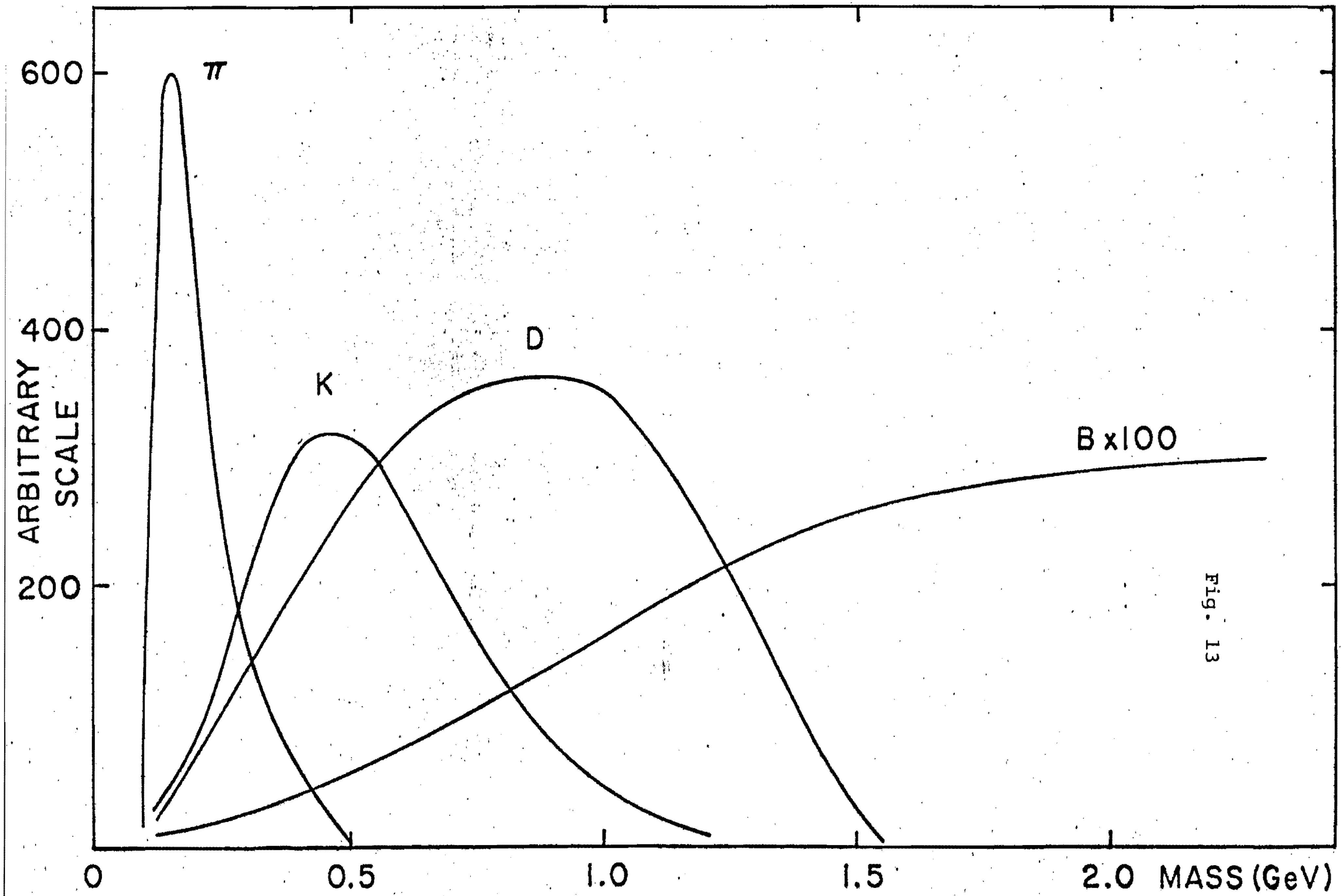

Fig. 13